

Research Article

How to cite this article: Asgharian Rezae F, Karimi M, Kamali H, Malaekheh-Nikouei B. Preparation and in-vitro characterization of triamcinolone acetonide-loaded lipid liquid crystal nanocarriers for ocular delivery. *Advanced Pharmaceutical Bulletin*, doi: 10.34172/apb.43671

Research Article

doi: 10.34172/apb.43671

## Preparation and in-vitro characterization of triamcinolone acetonide-loaded lipid liquid crystal nanocarriers for ocular delivery

Fatemeh Asgharian Rezae <sup>1,+</sup>, Malihe Karimi <sup>1,2,+</sup>, Hossein Kamali <sup>2,3 \*</sup>, Bizhan Malaekheh-Nikouei <sup>4,3\*</sup>

<sup>1</sup> Student Research Committee, School of Pharmacy, Mashhad University of Medical Sciences, Mashhad, Iran

<sup>2</sup> Targeted Drug Delivery Research Center, Pharmaceutical Technology Institute, Mashhad University of Medical Sciences, Mashhad, Iran.

<sup>3</sup> Department of Pharmaceutics, School of Pharmacy, Mashhad University of Medical Sciences, Mashhad, Iran.

<sup>4</sup> Nanotechnology Research Center, Pharmaceutical Technology Institute, Mashhad University of Medical Sciences, Mashhad, Iran.

+ **These authors contributed equally to this work**

\***Corresponding authors:**

**Hossein Kamali**, Targeted Drug Delivery Research Center, Pharmaceutical Technology Institute, Mashhad University of Medical Sciences, Mashhad, Iran; Tel: +98 51 31801302; Fax: +98 58 38823251, *Email*: kamalih@mums.ac.ir.

**Bizhan Malaekheh-Nikouei**, Nanotechnology Research Center, Pharmaceutical Technology Institute, Mashhad University of Medical Sciences, Mashhad, Iran, Mashhad, Iran; Tel: +98 51 31801302; Fax: +98 58 38823251, *Email*: Malaekhehb@mums.ac.ir

Asgharian Rezae : <https://orcid.org/0000-0002-7214-6864>

**Malaekheh-Nikouei** : <https://orcid.org/0000-0002-1908-9530>

**Running Title:** Triamcinolone-loaded lipid liquid crystal nanocarriers

### Declaration of Competing Interest

The authors declare that they have no conflict of interest

### Acknowledgments

The authors are grateful for the financial support provided by Mashhad University of Medical Sciences with IR.MUMS.PHARMACY.REC.1399.004 number.

### CRediT authorship contribution statement

**Fatemeh Asgharian Rezae:** Writing – original draft, Validation, Software, Methodology, Investigation, Formal analysis. **Malihe Karimi:** Writing – original draft, Supervision. **Hossein Kamali:** Writing – review & editing, Supervision, Methodology, Project administration, Funding acquisition, Conceptualization. **Bizhan Malaekheh-Nikouei:** Writing – review & editing, Supervision.

Submitted: August 28, 2024

Revised: November 20, 2024

Accepted: December 03, 2024

ePublished: December 05, 2024

## Abstract

**Purpose:** This study aimed to develop sustained-release Triamcinolone acetonide (TA) formulations using lipid liquid crystals (LLC) for ocular drug delivery and to characterize the designed formulations.

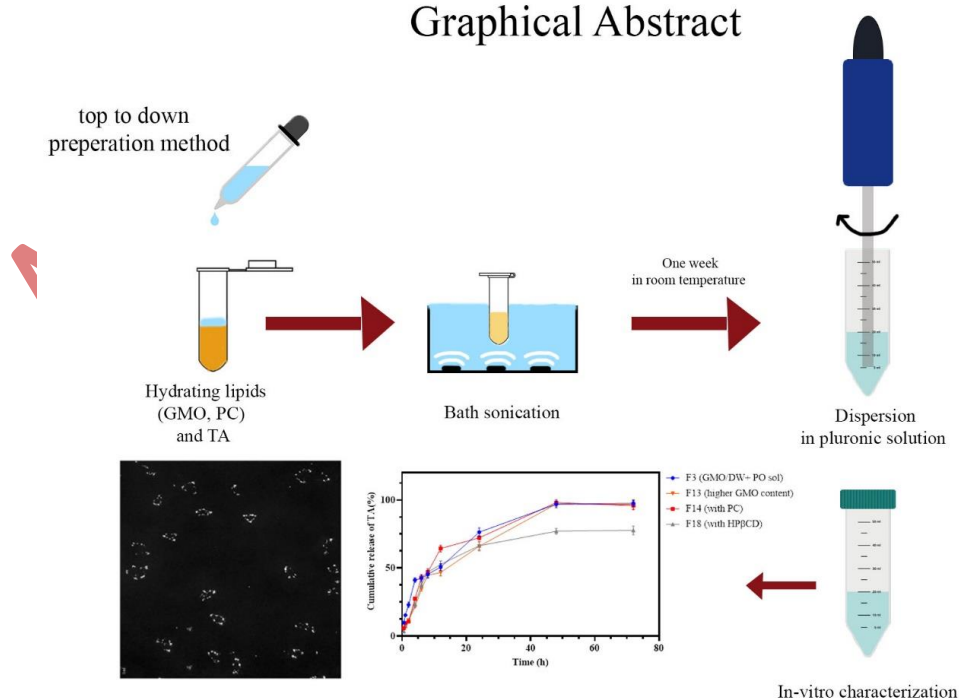
**Method:** Eighteen dispersed LLC formulations were prepared through a top-down approach, incorporating varying concentrations of TA and different proportions of glyceryl monooleate, deionized water, and Pluronic F127. An additional formulation comprising TA: HP $\beta$ CD complex was also developed to investigate the influence of hydroxypropyl beta-cyclodextrin (HP $\beta$ CD) on the properties of the formulations. The formulations were evaluated for their rheological properties in room temperature using a rheometer, syringeability by passing them through a 27G needle, size measurements via dynamic light scattering, and morphology through polarized light microscopy (PLM). Furthermore, the prepared formulations were injected into a dialysis tube and placed in a phosphate buffer at pH 7.4 and 37°C for in vitro release evaluation. Samples were taken at predetermined intervals and stored in a refrigerator until HPLC analysis. The percentage of Encapsulation efficacy and drug loading were evaluated using an indirect method. A reversed-phase HPLC method was employed to quantify the drug concentrations in the samples.

**Results:** All selected formulations demonstrated acceptable parameters, including particle size (less than 200 nm), polydispersity index ranging from 0.202 to 0.355, and zeta potential values between -14.3 and -32.8 mV. Additionally, the formulations showed good syringeability and achieved 100% drug release within 48 hours (except for the formulation containing HP $\beta$ CD). PLM analysis revealed the presence of hexosomes and cubosomes, indicating that an increase in hexosomes contributed to a more uniform drug release from the formulations.

**Conclusion:** Overall, the study findings suggest that liquid crystalline carriers can be a promising formulation for sustained ocular drug delivery of TA.

**Keywords:** Triamcinolone acetonide, Lipid liquid crystals, Nanocarriers, sustained-release formulations.

## Graphical Abstract



## 1. Introduction

Diseases affecting the posterior eye segment are the leading cause of blindness and vision impairment worldwide. Current treatments for these conditions include anti-angiogenesis agents and corticosteroids, such as triamcinolone acetonide (TA).<sup>1</sup> However, these prescribed medications face obstacles in effectively reaching the posterior segment of the eye. Topically administered therapies deliver only a minimal quantity to the posterior area, while systemic medications must traverse the blood-retina barrier. This passage often requires higher dosages, leading to increased side effects.<sup>2,3</sup> Intravitreal injection (IVI) is a highly effective method for delivering medication to the posterior segment of the eye. However, many patients find it undesirable due to its invasive nature, high costs, and potential complications associated with repeated injections. These side effects highlight the need for sustained-release formulations that can minimize the frequency of injections. Increasing the bioavailability of topical drugs can also pave the path to treating posterior eye segment disease using this comfortable and non-invasive method.<sup>4</sup>

TA is a relatively safe and effective conventional corticosteroid for treating ocular diseases that require long-term steroid therapy, such as diabetic cystoid macular edema, macular edema secondary to retinal vein occlusion, pseudophakic macular edema, uveitis, proliferative vitreoretinopathy, and exudative age-related macular degeneration.<sup>5</sup> However, delivering effective doses of TA to the posterior segment of the eye remains challenging. The conventional form of TA injected intravitreally is a 40 mg/ml suspension with the FDA-approved, preservative-free formulation, Triesence™, currently in the market.<sup>6</sup> Nevertheless, this form has complications of IVI such as increased intraocular pressure, hemorrhage, endophthalmitis, and cataract.<sup>7</sup> Efforts have been made to design novel topical formulations of TA to increase bioavailability of topical formations and alleviate the need for intraocular injections. Thus far, studies have been conducted on liposomes,<sup>8</sup> emulsomes,<sup>9</sup> nanocapsules,<sup>10</sup> PLGA-chitosan,<sup>11</sup> and poly-beta amino ester nanoparticles containing TA.<sup>12</sup> Furthermore, Topical Lipid-based nanoparticles have enhanced bioavailability due to higher residence time on the ocular surface and enhanced corneal penetration.<sup>13</sup>

LLC are lipid-based carriers that form by self-assembling amphiphilic molecules (i.e., certain lipids) in an aqueous environment. LLCs, based on solvent content (lyotropic) or temperature (thermotropic), appear in various phases and are capable of phase transition. Dispersed LLC are nanoparticles formed by high-energy dispersion of hydrated lipids in an aqueous solution (top to down) or controlled addition of a lipid solution to aqueous phase (down to top). Phases in dispersed LLC include lamellar, hexosomes, and cubosomes, which appear accordingly depending on the increase of solvent content, and reverse phases can also form by a change in the solvent's polarity.<sup>14</sup> The amphiphilic nature of LLC facilitates the loading of various drugs with a wide range of polarity. At the same time, the unique structures of lipidic regions and aqueous channels allow for the sustained release of loaded drugs. Furthermore, their lipidic nature enhances the penetration through various mucosa and cell membranes, resulting in a higher drug bioavailability.<sup>15</sup> Lipids used in LLCs are generally biocompatible, biodegradable, and readily available at a low cost.<sup>16</sup> These characteristics capacitate LLCs as valuable candidates for ocular drug delivery, either in the form of intraocular injection or topical application.

LLC-based formulations have shown superior performance in various drug formulations. Chen et al. developed a topical formulation of cyclosporin, that not only demonstrated no eye irritation or corneal damage but also indicated the potential of LLCs in reducing drug toxicity.<sup>14</sup> A cubosome formulation of flurbiprofen was found to have lower eye irritation and increased bioavailability.<sup>17</sup> Ketorolac-loaded cubosomes showed twice the corneal penetration compared to ketorolac solution and released the drug within 20 hours, while the plain solution fully released the drug in 2 hours.<sup>18</sup> Furthermore, Timolol maleate cubosomes had higher corneal penetration and retention time than the commercially available eye drops and lowered the intraocular pressure more effectively.<sup>19</sup>

LLC formulations have shown promise in sustained drug delivery and increasing the bioavailability of various drugs; however, dispersed LLC formulations of TA have yet to be investigated. In this study, we aimed to design and develop dispersed LLC formulations of TA and to evaluate them using various in-vitro methods.

## 2. Materials and method

### 2.1. Materials

Triamcinolone acetonide (TA) was purchased from Exir Pharmaceuticals, Iran. Glycerol monooleate (GMO) and phosphatidylcholine (PC) were all purchased from Tinab Shimi, Iran. HPLC grade solvents, including methanol, acetonitrile, and ethanol (96%), were purchased from second-hand providers, initially supplied by Deajung Chemicals & metals Co, Korea. Hydroxypropyl- $\beta$ -cyclodextrin (HP $\beta$ CD) and pluronic F127 were obtained from Shanghai Honglian Chemical Technology, China, and Merck, Germany, respectively.

### 2.2. Preparation of dispersed LLC formulations

According to the composition detailed in Table 1. The dispersed LLC formulations of TA were prepared using an up-to-down method.

First step: TA, GMO, and DW were weighed and initially mixed manually with a micro spatula. Subsequently, the mixture was further homogenized using a microtube shaker at 20,000 rpm for 5 minutes. The resulting formula was then subjected to bath sonication at 50°C for 30 minutes (Ultrasonic cleaner 2200 ETH S3, Soltec, Italy). In order to prevent lipid oxidation, the microtube containing the formulation was filled with nitrogen and sealed before any processing steps. The prepared formulations were then stabilized at room temperature (25°C) for one week (Figure 1). Additionally, three formulations (F14-16) were created by incorporating PC into the lipid phase to assess the impact of PC on the formulations.

Another method of preparation was also investigated. In this method, TA and GMO were initially physically mixed and bath-sonicated at 50°C for 30 minutes. After sonication, DW was added to the mixture without any additional mixing. The resulting formulation was then equilibrated at room temperature for a duration of one week. Subsequently, the impact of this method on the physicochemical properties of the formulations was analyzed, and the results were used to determine the optimal preparation method. The asterisk (\*) in Table 1 indicates the formulation prepared using this method.

Second step: Pluronic solution was prepared by adding 10 g of F127 to 100g of DW and keeping it in the refrigerator (8°C) for 20 minutes. Pluronic F127 can be solved in water either by heat or refrigerating as its solubility increases by either change in temperature.<sup>20</sup> The LLC gel prepared in the previous step was heated to 60°C and mixed with F127 solution. Next, the formula was homogenized at 2000 rpm for 10 minutes (Ultra-turbax IKA T110, IKA, China) and then probe sonicated using Soniprep 150 (MSE scientific, UK) at maximum power for 5 minutes (Table 1, Figure 1).

Two formulations (F17, F19) were prepared by adding HP $\beta$ CD to evaluate the effect of HP $\beta$ CD on drug release from the formulations. The choice of the cyclodextrin type was based on previous research.<sup>21</sup> First, TA was fully solubilized in 70% ethanol, while HP $\beta$ CD was dissolved in distilled water. These two solutions were mixed and left at room temperature for three days to allow for the solvents' evaporation. Simultaneously, a hydrated lipid mixture was prepared by mixing GMO and DW, followed by bath sonication at 50°C for 30 minutes. A week later, the F127 solution was added to the dried TA: HP $\beta$ CD mixture and bath sonicated at 30°C for 10 minutes to dissolve the drug: CD complex in the aqueous phase. The drug-free lipid liquid gel that was previously prepared was heated to 60°C and then mixed with the aqueous phase containing the TA: HP $\beta$ CD complex. Finally, the formulation was homogenized using the previously described method in the beginning of this section.

### 2.3. HPLC method for TA analysis

A stock solution of TA was prepared by solving TA in methanol (1 mg/ml) and later diluted to a series of concentrations ranging from 0.048 to 50  $\mu$ g/ml. These solutions were analyzed using the Shimadzu LC-20AD HPLC system (Shimadzu, Japan), connected to a UV/VIS



spectrophotometer (SPD-20AD) set at 254 nm. A Knauer reverse phase C18 4.6mm ID, Nucleosil-100, 150 mm column (Knauer, Germany) with a mobile phase of 40% acetonitrile, 60% deionized water, at a flow rate of 0.8 ml/min was used for chromatographic separation.<sup>22</sup> The injection volume was 20  $\mu$ l with column temperature set at 25°C. Subsequently, the equation for the calibration curve was obtained by plotting the absorbance peak areas of TA against the corresponding drug concentrations. The limit of detection (LOD) and Limit of Quantification (LOQ) were also calculated using the below formulas:<sup>23</sup>

$$\text{LOD} = \frac{3.3 \times \sigma}{S}$$

$$\text{LOQ} = \frac{10 \times \sigma}{S}$$

Where  $\sigma$  is the Standard deviation, and  $S$  is the slope of the drug's standard curve. The data below LOQ were removed from the calculations.

#### 2.4. Physicochemical characterization of dispersed LLC formulations

Dispersed formulations were selected for further assessment based on the amount of drug sediment observed and the overall appearance of each formulation.<sup>24</sup> Formulations that exhibited minimal drug sediment, highest possible drug loading, and a homogenous white appearance were chosen for additional assessment.

##### 2.4.1. Determination of particle size, size distribution, and zeta potential

The mean size, polydispersity index (PDI), and zeta potential of seven selected formulations were evaluated using dynamic light scattering (DLS) (Zetasizer nano-zs, Malvern Instruments, UK) at 25°C, with measurements conducted in triplicate. These seven samples were chosen to investigate how changes in various parameters affect the formulation. These parameters included alterations in drug concentration (F3, F4, F10), increasing GMO content (F13), addition of PC (F14, F16), and CD (F18).

##### 2.4.2. Measurement of Encapsulation efficacy and drug loading

The percentage of Encapsulation efficacy and drug loading were evaluated using an indirect method.<sup>24</sup> The selected formulations were centrifuged at 1500 rpm for 10 minutes (MIKRO 120 Hettich zentrifugen, ohne Rotor, Germany) to separate the unloaded drug.<sup>25</sup> Afterward, the formulations (supernatant liquid) and sediment were dissolved and diluted in methanol.<sup>26</sup> The diluted solutions were then analyzed for TA content using the previously described HPLC method by Wallace et al.<sup>27</sup> The encapsulation efficiency (EE%) and drug loading were calculated using the following formulas:

$$\text{Encapsulation} = \frac{D_{\text{total}} - D_{\text{unloaded}}}{D_{\text{total}}} \times 100$$

$$\text{Loading} = \frac{D_{\text{total}} - D_{\text{unloaded}}}{F_{\text{total}}} \times 100$$

Where  $D_{\text{total}}$  is the initial amount of TA in formulation,  $D_{\text{unloaded}}$  is the precipitated drug formulation, and  $F_{\text{total}}$  is the total weight of the formulation.

##### 2.4.3. Viscosity measurements and syringeability

The rheological behavior of the selected formulations was investigated using a Brookfield R/S plus (Brookfield, UK) in Rot stairs mode at 25°C, using a 3 ml steel cone. The formulations were exposed to 11 steps of continuous shear stress ranging from 0 to 100 Pa. Viscosity was measured using the power law set by the program. All measurements were carried out in triplicate. Moreover, all formulations were passed through a 27G needle syringe to assess their syringeability.

#### 2.5. Polarized light microscopy (PLM)

A microscope slide of a single drop of the selected formulations was prepared and subsequently analyzed using a polarized light microscope (Olympus BH2, Olympus Life Sciences, Japan) connected to a digital camera. This setup was used to evaluate the morphology of the prepared formulations.

#### 2.6. Measurement of TA solubility

Drug solubility is essential for determining the appropriate volume of the release study environment; therefore, an excess amount of TA was dissolved in PBS at pH 7.4 and

maintained at 37°C. The combination of TA: HPβCD in PBS was also evaluated to assess the effect of CDs on TA solubility. Samples were then centrifuged to separate any undissolved drug, and the supernatant was measured for drug content using the HPLC method. All samples were prepared and evaluated in triplicate.

### 2.7. In vitro release study of dispersed LLC formulations

The selected formulations were vortexed at 20,000 rpm for 5 minutes prior to injection to ensure no sediment remained in the formulation. A 12KD dialysis tube was cut into 5 cm pieces and tied on one end. Then, 3 ml of the dispersed formulation was then injected into the tube and sealed on the other end. The tube was placed in 120 ml of PBS (pH 7.4) at 37°C and shaken in a shaking water bath (Shimaz, Iran) at 40 rpm. Approximately 0.5 ml of the release environment was sampled at predetermined time points (1, 2, 4, 6, 8, 12, 24, 36, and 48 hours) and replaced with an equal volume of PBS to maintain the sink condition. The samples were then refrigerated until they were measured for TA content using HPLC.

### 2.8. Statistical analysis

The results were analyzed using GraphPad Prism 10, and related graphs were also drawn as needed. To compare release similarity between formulations, the similarity factor ( $f_2$ ) was calculated based on previous research.<sup>28</sup> An ordinary one-way ANOVA with Tukey's multiple comparison test was utilized as required, and p values less than 0.05 were considered statistically significant.

$$f_2 = 50 \log \left\{ \left[ 1 + \frac{1}{n} \sum_{t=1}^n (R_t - T_t)^2 \right]^{-0.5} \times 100 \right\}$$

## 3. Results

### 3.1. Calibration curve of TA

The calibration curve of TA showed linearity in the range of 0.39 to 50 µg/ml with a regression value of 0.995 (Figure 2A). The chromatogram of 50 µg/ml concentration of TA in methanol is shown in Figure 2B, with a retention time of 5.29 minutes in methanol and 6.15 in PBS (PH 7.4). Furthermore, an example of release sample analysis is presented in Figure 2C. The peaks observed in both chromatograms are sharp and with an acceptable retention time. Moreover, the other peaks observed in Figure 2 may represent buffer, NMP, and lipid peaks as this is a release sample analysis and contains all mentioned substances. The calculated LOD and LOQ were 0.132 µg/mL and 0.402 µg/mL, accordingly.

### 3.2. Physicochemical characterization of dispersed LLC formulations

Four dispersed formulations (F3, F13, F14, F18) were selected for further evaluation based on the amount of drug sediment and the overall appearance of the formulation.<sup>24</sup> These selected formulations had the maximum possible drug loading with the minimum amount of drug sediment and a homogenous white appearance as shown in Figure 1.

#### 3.2.1. Dynamic light scattering

Seven formulations were chosen to investigate the effects of various parameters on their characteristics. These parameters included changes made in drug concentration (F3, F4, F10), increasing GMO content (F13), addition of PC (F14, F16), and CD (F18). The DLS results of these formulations, mean size measurements, zeta potential, and PDI, are shown in Table 2 and Appendix I. A comparison of the particle size between various formulations is also shown in Figure 3A. Furthermore, an example of a sample PDI diagram is presented in Figure 3B.

The particle sizes of the designed formulations were found to vary between 89.01±0.21 and 141.10±0.31 nm, which are all within the acceptable nanoparticle range,<sup>29</sup> with a PDI of 0.202-0.356. Furthermore, increases in drug content (F3, F4, and F10), the addition of CDs (F18), increases in lipid concentration (F13), and the addition of PC (F14, F16) to the formulations considerably increased the mean particle size. However, the addition of CDs had a less considerable impact. The other preparation method (formulations marked with asterisk\*) used

to produce the formulation also increased particle size and, therefore, was no longer used to develop dispersed formulations in this study.

Furthermore, it was observed that the PDI increases with higher drug concentration (F10), an increase in lipid content (F3), and the addition of phosphatidylcholine to the formulation (F14, 16).

### 3.2.2. Encapsulation and loading measurements

The Encapsulation Efficacy and drug loading of the selected formulations were measured, and the sediment in each formulation represents the unloaded drug (Table 3).<sup>25</sup>

The objective of designing nanocarriers is to reach the maximum possible loading and encapsulation efficacy. According to the loading and EE% measurements, F3 and F18 (containing HP $\beta$ CD) demonstrated the best results in comparison, and can be considered optimal. It was noted that increasing the content of GMO (F13) and adding PC (F14) led to a reduction in both drug loading and EE%. However, the centrifugation process used to separate the unloaded drug may have affected the results.

### 3.2.3. Viscosity measurements and syringeability of dispersed LLC formulations

The viscosity diagrams of all selected formulations at 25°C, and the viscosity diagram of F3 at corneal temperature (34°C)<sup>30</sup> are shown in Figure 4.

All formulations exhibited pseudoplastic behavior, where the viscosity decreases with increased shear stress in a non-linear pattern.<sup>31</sup> This feature can be favorable in designing topical formulations in the form of eye drops, as the viscosity decreases when applying the eye drop by increasing users' pressure on the container. When applied, the lack of external pressure results in higher viscosity and helps retain the formulation in the applied location.<sup>32</sup> An increase in viscosity was also observed by increasing temperature, which can be helpful as the higher viscosity stabilizes the formulation in place and prevents the dispersion of the medicine when applied topically. Furthermore, the addition of PC also increases the viscosity, which can be due to the physicochemical characteristics of phosphatidylcholine and its intrinsic high viscosity and melting point.

### 3.3. Triamcinolone acetate solubility

The solubility of TA and TA: HP $\beta$ CD complex in PBS was measured at  $24.66 \pm 0.25$  and  $153.74 \pm 0.32$   $\mu\text{g/ml}$ , respectively. The solubility results were used to calculate the suitable volume of the release medium needed to maintain the synchronization conditions, which should be capable of solubilizing 2-10 times the whole drug content in the release medium.<sup>33</sup> As anticipated, the addition of CDs considerably increased the drug solubility of TA, which is only sparingly soluble in aqueous buffers. It is well established that CDs are commonly employed to increase the solubility of such drugs in aqueous environments.<sup>21</sup>

### 3.5. Polarized light microscopy (PLM) photography

The images of dispersed LLC formulations captured using PLM are displayed in Figure 5. It has been observed that LLC appear in 2 forms in PLM photography: isotropic (i.e., Cubosome) which allows all light to pass through and appears entirely black, while anisotropic (i.e., hexosome, lamellar) which reflect light and appears as bright crystals.<sup>34</sup> As shown in Figure 5, the F13 formulation exhibits the highest number of bright crystals (anisotropic forms), while F3 is predominantly in the isotropic state (cubosomes). Additionally, the phases present in dispersed LLC significantly influence the formulations' release, loading, and overall characteristics.

### 3.4. In-vitro release of dispersed formulations

The drug release results from dispersed formulations are represented in Figure 6. All formulations, except for F18, released their entire drug content within 48 hours. In contrast, F18 did not fully release its drug content even after 72 hours. It was observed that F13 showed slower and more consistent drug release, while formulations F3 and F14 displayed a burst release and sudden changes in their release profiles, respectively. In order to facilitate comparison of drug release among various formulations, the similarity factor ( $f_2$ ) was calculated using the formula described in the methods section (Table 4). Research has shown

that the similarity factor indicates the likeness of drug release from different formulations, with values above 50 suggesting a similarity in release profiles at a specific time. As illustrated in Table 4, F18 (containing HP $\beta$ CD) has demonstrated a significant difference in release compared to all other formulations over the past 48 hours. Specifically, it differs from formulation F3 at 2 and 4 hours. In order to investigate the burst release from various formulations, data from the first 6 hours were analyzed separately for f2 using Ordinary One-way ANOVA and Tukey's multiple comparison test. The findings are presented in Table 5. To effectively understand the results of the similarity factor, one side is designated as the base, while the others are compared against it. For instance, in the comparison of f2 (F3-F18) with f2 (F18-F13), F18 serves as the base. In this case, we compare formulations F3 and F13. The results indicate that F13, which has a higher GMO content, and F18, which contains HP $\beta$ CD, exhibit lower burst release rates compared to F3, with a p-value of less than 0.05.

### 3.6. Optimum dispersed formulation

Based on the results from the conducted *in vitro* examinations, the F13 formulation was selected as the optimal formulation. This decision was made because it demonstrated complete drug release within two days, along with a slow and steady release profile attributed to the highest formation of hexagonal LLC. Conversely, F18 exhibited incomplete drug release, likely due to the formation of the drug CD sediment, and therefore was not chosen. Additionally, F14 displayed a more irregular drug release pattern, and F3 had a higher burst release compared to F13 formulation.

## 4. Discussion

Diseases of the posterior eye segment are among the leading causes of eye impairment and blindness worldwide. Treatment for these conditions primarily relies on corticosteroids and antiangiogenic agents.<sup>35</sup> However, the topical application of these medications exhibits minimal absorption in the posterior parts of the eye. Additionally, the presence of the blood-retinal barrier poses a significant challenge to the absorption of drugs administered systemically. While intraocular injections are highly effective, this method is invasive, costly, and complex, which can lead to decreased patient compliance.<sup>2,3,36</sup> Therefore, it seems necessary to design and manufacture sustained-release formulations. Moreover, designing topical formulations with higher bioavailability can reduce the need for invasive methods, thereby enhancing patients' compliance and the ease of medication administration. In this study, we designed dispersed lipid liquid crystal (LLC) formulations of triamcinolone acetonide (TA) that can provide a sustained release of TA over a period of 48 hours.

Dispersed LLC systems can be suitable for designing sustained-release intraocular drug delivery due to their ease of injection, pseudoplastic rheological behavior, and reduced drug toxicity. Furthermore, the lipids used in these formulations are biodegradable, eliminating the need for surgery to remove any remnants from the eye.<sup>16</sup> Moreover, the amphiphilic structure of their compounds allows the loading of various drugs regardless of their polarity. Studies have been conducted on dispersed LLCs of several drugs, such as ondansetron,<sup>24</sup> ketorolac,<sup>18</sup> cyclosporin,<sup>37</sup> timolol,<sup>19</sup> and vancomycin.<sup>38</sup> However, dispersed formulations typically exhibit a rapid drug release, often reach maximum release within 24 - 72 hours. Therefore, using these formulations in a topical form is a more favorable option.

Moreover, the dispersed formulation's lower viscosity and liquid form make it easier to use as eye drops. Although there are differences between *in-vivo* and *in-vitro* drug release due to the higher viscosity of the vitreous humor and the unique conditions of the internal environment of the eye,<sup>39</sup> *in-vivo* studies also confirm this release pattern. Therefore, such formulations should be considered primarily as a topical drug delivery option. Furthermore, unlike other diacyl lipids, GMO LLC phases dissolve more quickly in aqueous environments and can exchange monomer lipids with other biological structures. This ability disrupts biological membranes and enhances penetration, improving the application of the GMO-based dispersed LLC in eye drops.<sup>26</sup>



The lipid GMO can form cubic and hexagonal phases depending on the amount of solvent and temperature. In physiological conditions and excess water, the cubic phase formation is more commonly observed,<sup>40</sup> which can also be seen in polarized light microscopy (PLM) images. Similarly, in dispersed formulations made of GMO, water, and pluronic F127 for the drugs simvastatin, oral indomethacin, and ophthalmic sertaconazole,<sup>32</sup> the predominance of the cubic phase has been demonstrated.<sup>41</sup> However, as the lipophilicity of the formulation increases due to a higher concentration of GMO (sample F13), the amount of water in the medium decreases, leading to the formation of a hexagonal phase. These results align with the study conducted by Salonen et al., which found that in self-assembled monoglyceride-based dispersions at room temperature with excess water, an increase in oil content results in the formation of cubic and hexagonal phases.<sup>42</sup> On the other hand, phosphatidylcholine (PC) in the LLC structure primarily tends to form a lamellar phase. This tendency can be affected by the presence of other lipids in the formulation.<sup>43</sup> With the addition of PC to the dispersed formulation (F14 sample), lamellar formations can be observed in the PLM images.

Among the dispersed LLC, hexosomes release the drug slowly and continuously due to their limited aqueous channels. In contrast, cubosomes, which have a higher solvent content and more extensive aqueous channels, provide a relatively faster drug release.<sup>40</sup> With an increase in lipid percentage in the F13 sample, resulting in the formation of hexosomes, we observe less burst release and a more uniform drug release process compared to the F3 formulation, which has a lower content of GMO. Similarly, a study involving Vancomycin dispersed LLC found that the release from the hexagonal phase was prolonged in simulated tear fluid, unlike that from the cubic phase. This was attributed to the hexagonal phase's two-dimensional symmetry and its closed water channels, which create a complex diffusion route that facilitates the gradual release of the trapped molecule.<sup>38</sup> On the other hand, the PC lamellar phase tends to change depending on the content of water, other lipids, and even the amount of drug in the formulation,<sup>40,43</sup> and this matter affects the drug release from PC-containing LLC formulations. As seen in sample F14, the release pattern is somewhat irregular, which can be a sign of the phase change of the formulation following the alterations made during the drug release process.

Cyclodextrins (CDs) feature a hydrophobic inner core and a hydrophilic outer shell, primarily used to enhance the solubility of insoluble drugs in aqueous environments. The application of CDs in ophthalmic formulations has been explored in numerous studies, with hydroxypropyl beta-cyclodextrin (HP $\beta$ CD) being utilized in the development of formulations containing dexamethasone, fluorometholone, and fluocinolone.<sup>44</sup> Additionally, a separate study investigated the enhancement of triamcinolone acetonide (TA) solubility using HP $\beta$ CD. This study demonstrated that a molar ratio of 1:7 (drug: CD) resulted in a homogeneous molecular structure, whereas a lower drug-to-CD ratio led to the formation of drug crystals measuring 10 to 15 microns.<sup>21</sup> Due to the impracticality of employing a 1:7 molar ratio of drug to CD (which would require 124 grams of CD for a total formulation mass of only 10 grams), the reduced quantities of CD used are likely to promote crystal formation alongside the drug. This crystallization may contribute to the lower release rates observed in the F18 formulation. The F18 formulation shows higher loading and encapsulation, but the decreased release further supports this hypothesis.

Our designed formulations exhibited particle sizes ranging from  $89.01 \pm 0.21$  nm to  $141.1 \pm 0.31$  nm, all of which fall within the acceptable nanoparticle range. The polydispersity index (PDI) ranged from 0.202 to 0.356. Particle sizes smaller than 200 nm are known to penetrate the cornea effectively, making them ideal for ophthalmic formulations.<sup>45</sup> In comparison, our particle sizes were significantly smaller than those reported in studies on diclofenac sodium,<sup>46</sup> latanoprost,<sup>47</sup> and sertaconazole<sup>32</sup> cubosomes with particles size ranging between  $409 \pm 3.0$  to  $679 \pm 2.0$  nm,  $204.6 \pm 1.6$  to  $217.8 \pm 19.6$  nm, and  $125.10 \pm 1.41$  to  $383.50 \pm 7.78$  nm, respectively. The preparation method plays a crucial role in determining the particle size of dispersed LLC formulations. Formulations created using a bottom-up approach often yield

larger particle sizes.<sup>46</sup> In our study, we observed that a simple change in production method and removal of a single homogenizing step resulted in larger particle size (F3 vs. F4). The PDI increases with higher drug concentrations (F10), an increase in lipid content (F3), and the addition of phosphatidylcholine (PC) to the formulation (F14, 16). The increased viscosity resulting from the addition of PC could interfere with the homogenization process, leading to larger particle sizes. Younes et al. suggested that a higher concentration of lipid phase could cause aggregation of the formed nanoparticles,<sup>32</sup> which was further confirmed by a study conducted by Malaekheh et al. on fluorometholone cubosomes.<sup>48</sup> Additionally, a higher drug concentration and the inclusion of HP $\beta$ CD, specifically with TA, could also result in particle aggregation since TA naturally tends to form crystals.<sup>49</sup> The literature has already established the formation of TA: HP $\beta$ CD complexes.<sup>21</sup> Furthermore, a zeta potential greater than 20 mV or less than -20 mV is considered optimal for preventing aggregation.<sup>50</sup> Almost all our selected dispersed formulations (F3, F13, F18) exhibited zeta potentials within this optimal range. Our study was the first to develop a dispersed LLC formulation of TA and to evaluate impact of adding HP $\beta$ CD on the physicochemical characteristics and drug release from this formulation. We successfully produced a number of formulations and explored how variations in the preparation method, drug concentration, and types of lipids affected the LLC formulations. Unfortunately, performing in-vivo examinations was not feasible in our study. Future research could focus on assessing the safety and efficacy of these formulations in retinal cell lines and rabbit eyes. Furthermore, long-term stability studies were not conducted, which can also be considered in future work.

#### 4. Conclusion

In this study, sustained-release formulations of TA were prepared using a dispersed LLC system for ocular use to overcome the disadvantages of traditional drug forms. The optimum formulation, F13 (6.3% w/w GMO, 91% pluronic F127), with a drug concentration of 0.05% w/w, released its total drug content within 48 hours. The formation of hexosomes was observed in this formulation, which resulted in a more uniform drug release. Considering the unique characteristics of LLCs, these formulations can treat various eye diseases requiring corticosteroid treatment.

To the best of the authors' knowledge, this study was a comprehensive pilot research on developing a dispersed LLC formulation of TA. The research also evaluated the impact of adding hydroxypropyl-beta-cyclodextrin (HP $\beta$ CD) on the physicochemical properties and drug release characteristics of this formulation. A satisfactory number of formulations were produced in this research, and the effects of variations in the preparation method, drug concentration, and lipid composition on the LLC formulations were also investigated. Given the potential of topical lipid-based nanoparticles for their enhanced bioavailability and biocompatibility, this formulation should be considered for further research in ocular drug delivery. However, in-vivo examinations could not be conducted in this study due to constraints. Thus, future research may focus on assessing the safety and efficacy of these formulations in retinal cell lines and rabbit models. Furthermore, long-term stability studies were not conducted, which can also be considered in future work.

#### 5. Competing Interest

The authors declare that they have no conflict of interest

#### 6. Funding

The authors are grateful for the financial support provided by Mashhad University of Medical Sciences with 991984 number.

#### 7. Authors' contributions

**Fatemeh Asgharian Rezae:** Writing – original draft, Validation, Software, Methodology, Investigation, Formal analysis. **Malihe Karimi:** Writing – original draft, Supervision. **Hossein Kamali:** Writing – review & editing, Supervision, Methodology, Project administration, Funding acquisition, Conceptualization. **Bizhan Malaekheh-Nikouei:** Writing – review & editing, Supervision.

## 8. Ethics Statement

All experiments were authorized by the institutional research ethics committee at Mashhad University of Medical Sciences with IR.MUMS.PHARMACY.REC.1399.004 number.

## 9. Data Availability

The datasets generated during and/or analyzed during the current study are available from the corresponding author upon request.

## 10. Consent for publication

All authors approved for publication.

## References

1. Cabrera FJ, Wang DC, Reddy K, Acharya G, Shin CS. Challenges and opportunities for drug delivery to the posterior of the eye. *Drug discovery today* 2019;24(8):1679-84. doi: <https://doi.org/10.1016/j.drudis.2019.05.035>
2. Choonara YE, Pillay V, Danckwerts MP, Carmichael TR, Du Toit LC. A review of implantable intravitreal drug delivery technologies for the treatment of posterior segment eye diseases. *Journal of pharmaceutical sciences* 2010;99(5):2219-39. doi: <https://doi.org/10.1002/jps.21987>
3. Hughes PM, Olejnik O, Chang-Lin J-E, Wilson CG. Topical and systemic drug delivery to the posterior segments. *Advanced drug delivery reviews* 2005;57(14):2010-32. doi: <https://doi.org/10.1016/j.addr.2005.09.004>
4. Yadav D, Varma LT, Yadav K. Drug delivery to posterior segment of the eye: conventional delivery strategies, their barriers, and restrictions. *Drug Delivery for the Retina and Posterior Segment Disease* 2018:51-67. doi: [https://doi.org/10.1007/978-3-319-95807-1\\_3](https://doi.org/10.1007/978-3-319-95807-1_3)
5. Gaballa SA, Kompella UB, Elgarhy O, Alqahtani AM, Pierscionek B, Alany RG, Abdelkader H. Corticosteroids in ophthalmology: Drug delivery innovations, pharmacology, clinical applications, and future perspectives. *Drug Delivery and Translational Research* 2021;11:866-93. doi: <https://doi.org/10.1007/s13346-020-00843-z>
6. Triesence. <https://www.accutome.com/triesence-injectable-40mg-1ml-preservative-free> [updated 26/2; cited 2024 26/2]; Available from: <https://www.accutome.com/triesence-injectable-40mg-1ml-preservative-free>.
7. Jager RD, Aiello LP, Patel SC, Cunningham Jr ET. Risks of intravitreal injection: a comprehensive review. *Retina* 2004;24(5):676-98.
8. Li J, Cheng T, Tian Q, Cheng Y, Zhao L, Zhang X, Qu Y. A more efficient ocular delivery system of triamcinolone acetonide as eye drop to the posterior segment of the eye. *Drug delivery* 2019;26(1):188-98. doi: <https://doi.org/10.1080/10717544.2019.1571122>
9. Kapadia R, Parikh K, Jain M, Sawant K. Topical instillation of triamcinolone a cetonide-loaded emulsomes for posterior ocular delivery: statistical optimization and in vitro-in vivo studies. *Drug Delivery and Translational Research* 2021;11:984-99. doi: <https://doi.org/10.1007/s13346-020-00810-8>
10. Formica ML, Gamboa GU, Tártara L, Luna J, Benoit J, Palma SD. Triamcinolone acetonide-loaded lipid nanocapsules for ophthalmic applications. *International journal of pharmaceutics* 2020;573:118795. doi: <https://doi.org/10.1016/j.ijpharm.2019.118795>

11. Xing Y, Zhu L, Zhang K, Li T, Huang S. Nanodelivery of triamcinolone acetonide with PLGA-chitosan nanoparticles for the treatment of ocular inflammation. *Artificial Cells, Nanomedicine, and Biotechnology* 2021;49(1):308-16. doi: <https://doi.org/10.1080/21691401.2021.1895184>
12. Sabzevari A, Adibkia K, Hashemi H, De Geest BG, Mohsenzadeh N, Atyabi F, et al. Improved anti-inflammatory effects in rabbit eye model using biodegradable poly beta-amino ester nanoparticles of triamcinolone acetonide. *Investigative ophthalmology & visual science* 2013;54(8):5520-6. doi: <https://doi.org/10.1167/iovs.13-12296>
13. Navarro-Partida J, Castro-Castaneda CR, Santa Cruz-Pavlovich FJ, Aceves-Franco LA, Guy TO, Santos A. Lipid-based nanocarriers as topical drug delivery systems for intraocular diseases. *Pharmaceutics* 2021;13(5):678. doi: <https://doi.org/10.3390/pharmaceutics13050678>
14. Chavda VP, Dyawanapelly S, Dawre S, Ferreira-Faria I, Bezbaruah R, Gogoi NR, et al. Lyotropic liquid crystalline phases: drug delivery and biomedical applications. *International Journal of Pharmaceutics* 2023;647:123546. doi: <https://doi.org/10.1016/j.ijpharm.2023.123546>
15. Zabara A, Mezzenga R. Controlling molecular transport and sustained drug release in lipid-based liquid crystalline mesophases. *Journal of Controlled Release* 2014;188:31-43. doi: <https://doi.org/10.1016/j.jconrel.2014.05.052>
16. Singhvi G, Banerjee S, Khosa A. Chapter 11 - Lyotropic liquid crystal nanoparticles: A novel improved lipidic drug delivery system. In: Grumezescu AM, editor. *Organic Materials as Smart Nanocarriers for Drug Delivery*: William Andrew Publishing; 2018. p. 471-517.
17. Han S, Shen J-q, Gan Y, Geng H-m, Zhang X-x, Zhu C-l, Gan L. Novel vehicle based on cubosomes for ophthalmic delivery of flurbiprofen with low irritancy and high bioavailability. *Acta Pharmacologica Sinica* 2010;31(8):990-8. doi: <https://doi.org/10.1038/aps.2010.98>
18. Ali Z, Sharma PK, Warsi MH. Fabrication and evaluation of ketorolac loaded cubosome for ocular drug delivery. *Journal of applied pharmaceutical science* 2016;6(9):204-8. doi: <https://doi.org/10.1038/aps.2010.98>
19. Huang J, Peng T, Li Y, Zhan Z, Zeng Y, Huang Y, et al. Ocular cubosome drug delivery system for timolol maleate: preparation, characterization, cytotoxicity, ex vivo, and in vivo evaluation. *Aaps Pharmscitech* 2017;18:2919-26. doi: <https://doi.org/10.1208/s12249-017-0763-8>
20. Higuchi A. Separation and Purification of Stem and Blood Cells by Porous Polymeric Membranes. 2010.
21. Miro A, Ungaro F, Balzano F, Masi S, Musto P, La Manna P, et al. Triamcinolone solubilization by (2-hydroxypropyl)- $\beta$ -cyclodextrin: A spectroscopic and computational approach. *Carbohydrate polymers* 2012;90(3):1288-98. doi: <https://doi.org/10.1016/j.carbpol.2012.06.075>
22. Sheshala R, Hong GC, Yee WP, Meka VS, Thakur RRS. In situ forming phase-inversion implants for sustained ocular delivery of triamcinolone acetonide. *Drug delivery and translational research* 2019;9:534-42. doi: <https://doi.org/10.1007/s13346-018-0491-y>
23. Armbruster DA, Pry T. Limit of blank, limit of detection and limit of quantitation. *The clinical biochemist reviews* 2008;29(Suppl 1):S49. doi: PMC2556583
24. Mansour M, Kamel A, Mansour S, Mortada N. Novel polyglycerol-dioleate based cubosomal dispersion with tailored physical characteristics for controlled delivery of ondansetron. *Colloids and Surfaces B: Biointerfaces* 2017;156:44-54. doi: <https://doi.org/10.1016/j.colsurfb.2017.04.052>
25. Daneshmand S, Golmohammadzadeh S, Jaafari MR, Movaffagh J, Rezaee M, Sahebkar A, Malaekheh-Nikouei B. Encapsulation challenges, the substantial issue in solid lipid nanoparticles characterization. *Journal of cellular biochemistry* 2018;119(6):4251-64. doi: <https://doi.org/10.1002/jcb.26617>
26. Barauskas J, Cervin C, Jankunec M, Špandryeva M, Ribokaitė K, Tiberg F, Johnsson M. Interactions of lipid-based liquid crystalline nanoparticles with model and cell membranes.



- International journal of pharmaceuticals* 2010;391(1-2):284-91. doi: <https://doi.org/10.1016/j.ijpharm.2010.03.016>
27. Wallace SJ, Li J, Nation RL, Boyd BJ. Drug release from nanomedicines: selection of appropriate encapsulation and release methodology. *Drug delivery and translational research* 2012;2:284-92. doi: <https://doi.org/10.1007/s13346-012-0064-4>
28. Chen Y, Liang X, Ma P, Tao Y, Wu X, Wu X, et al. Phytantriol-based in situ liquid crystals with long-term release for intra-articular administration. *Aaps Pharmscitech* 2015;16:846-54. doi: <https://doi.org/10.1208/s12249-014-0277-6>
29. Rizvi SA, Saleh AM. Applications of nanoparticle systems in drug delivery technology. *Saudi pharmaceutical journal* 2018;26(1):64-70. doi: <https://doi.org/10.1016/j.jsps.2017.10.012>
30. Kessel L, Johnson L, Arvidsson H, Larsen M. The relationship between body and ambient temperature and corneal temperature. *Investigative ophthalmology & visual science* 2010;51(12):6593-7. doi: <https://doi.org/10.1167/iovs.10-5659>
31. Tatsuoka F, Di Benedetto H, Enomoto T, Kawabe S, Kongkitkul W. Various viscosity types of geomaterials in shear and their mathematical expression. *Soils and Foundations* 2008;48(1):41-60. doi: <https://doi.org/10.3208/sandf.48.41>
32. Younes NF, Abdel-Halim SA, Ellassasy AI. Corneal targeted Sertaconazole nitrate loaded cubosomes: preparation, statistical optimization, in vitro characterization, ex vivo permeation and in vivo studies. *International journal of pharmaceuticals* 2018;553(1-2):386-97. doi: <https://doi.org/10.1016/j.ijpharm.2018.10.057>
33. Jug M, Hafner A, Lovrić J, Kregar ML, Pepić I, Vanić Ž, et al. An overview of in vitro dissolution/release methods for novel mucosal drug delivery systems. *Journal of pharmaceutical and biomedical analysis* 2018;147:350-66. doi: <https://doi.org/10.1016/j.jpba.2017.06.072>
34. Dierking I, Al-Zangana S. Lyotropic liquid crystal phases from anisotropic nanomaterials. *Nanomaterials* 2017;7(10):305. doi: <https://doi.org/10.3390/nano7100305>
35. Edelhauser HF, Rowe-Rendleman CL, Robinson MR, Dawson DG, Chader GJ, Grossniklaus HE, et al. Ophthalmic drug delivery systems for the treatment of retinal diseases: basic research to clinical applications. *Investigative ophthalmology & visual science* 2010;51(11):5403-20. doi: <https://doi.org/10.1167/iovs.10-5392>
36. Hsu J. Drug delivery methods for posterior segment disease. *Current opinion in ophthalmology* 2007;18(3):235-9. doi: 10.1097/ICU.0b013e3281108000
37. Chen Y, Ma P, Gui S. Cubic and hexagonal liquid crystals as drug delivery systems. *BioMed research international* 2014;2014.
38. Milak S, Chemelli A, Glatter O, Zimmer A. Vancomycin ocular delivery systems based on glycerol monooleate reversed hexagonal and reversed cubic liquid crystalline phases. *European Journal of Pharmaceutics and Biopharmaceutics* 2019;139:279-90. doi: <https://doi.org/10.1016/j.ejpb.2019.04.009>
39. El-Kamel A. In vitro and in vivo evaluation of Pluronic F127-based ocular delivery system for timolol maleate. *International journal of pharmaceuticals* 2002;241(1):47-55. doi: [https://doi.org/10.1016/S0378-5173\(02\)00234-X](https://doi.org/10.1016/S0378-5173(02)00234-X)
40. Tiberg F, Johnsson M. Drug delivery applications of non-lamellar liquid crystalline phases and nanoparticles. *Journal of Drug Delivery Science and Technology* 2011;21(1):101-9. doi: [https://doi.org/10.1016/S1773-2247\(11\)50009-7](https://doi.org/10.1016/S1773-2247(11)50009-7)
41. Báez-Santos YM, Otte A, Mun EA, Soh B-K, Song C-G, Lee Y-n, Park K. Formulation and characterization of a liquid crystalline hexagonal mesophase region of phosphatidylcholine, sorbitan monooleate, and tocopherol acetate for sustained delivery of leuprolide acetate. *International journal of pharmaceuticals* 2016;514(1):314-21. doi: <https://doi.org/10.1016/j.ijpharm.2016.06.138>

42. Salonen A, Guillot S, Glatter O. Determination of water content in internally self-assembled monoglyceride-based dispersions from the bulk phase. *Langmuir* 2007;23(18):9151-4. doi: <https://doi.org/10.1021/la7015319>
43. Martiel I, Sagalowicz L, Mezzenga R. Phospholipid-based nonlamellar mesophases for delivery systems: Bridging the gap between empirical and rational design. *Advances in colloid and interface science* 2014;209:127-43. doi: <https://doi.org/10.1016/j.cis.2014.03.005>
44. Loftsson T, Stefánsson E. Cyclodextrins and topical drug delivery to the anterior and posterior segments of the eye. *International journal of pharmaceutics* 2017;531(2):413-23. doi: <https://doi.org/10.1016/j.ijpharm.2017.04.010>
45. Baba K, Tanaka Y, Kubota A, Kasai H, Yokokura S, Nakanishi H, Nishida K. A method for enhancing the ocular penetration of eye drops using nanoparticles of hydrolyzable dye. *Journal of controlled release* 2011;153(3):278-87. doi: <https://doi.org/10.1016/j.jconrel.2011.04.019>
46. Hundekar YR, Saboji J, Patil S, Nanjwade B. Preparation and evaluation of diclofenac sodium cubosomes for percutaneous administration. *World J Pharm Pharm Sci* 2014;3(5):523-39.
47. Bessone CDV, Akhlaghi SP, Tártara LI, Quinteros DA, Loh W, Allemandi DA. Latanoprost-loaded phytantriol cubosomes for the treatment of glaucoma. *European journal of pharmaceutical sciences* 2021;160:105748. doi: <https://doi.org/10.1016/j.ejps.2021.105748>
48. Malaekheh-Nikouei B, Vafaei F, Karimi M, Nosrati R, Kamali H. Preparation and in-vitro evaluation of fluorometholone cubosomes for ocular delivery. *Nanomedicine Journal* 2023;10(4). doi: DOI: 10.22038/NMJ.2023.73985.1801
49. Wang J-R, Zhu B, Zhang Z, Bao J, Deng G, Ding Q, Mei X. Polymorphism of triamcinolone acetonide acetate and its implication for the morphology stability of the finished drug product. *Crystal Growth & Design* 2017;17(6):3482-90. doi: <https://doi.org/10.1021/acs.cgd.7b00453>
50. Honary S, Zahir F. Effect of zeta potential on the properties of nano-drug delivery systems- a review (Part 1). *Tropical journal of pharmaceutical research* 2013;12(2):255-64. doi: 10.4314/tjpr.v12i2.20

### Figure Captions

**Figure 1.** Appearance of the dispersed LLC formulations. (A) First step: TA, GMO, and DW were weighed and mixed, (B) Second step: The LLC gel prepared in the previous step was mixed with F127 solution.

**Figure 2.** (A) HPLC standard curve and chromatograms of TA. (B) HPLC chromatogram of TA (50 µg/ml) in methanol, (C) HPLC chromatogram of TA in PBS (F13 release sample at 6 h).

**Figure 3.** (A) Particle size comparison of dispersed formulations, (B) Size distribution diagram of F3 dispersed LLC formulation.

**Figure 4.** Viscosity diagram of selected dispersed LLC formulations. (A) F14, (B) F3, (C) F13, (D) F18, (E) F3 in 34 degrees °C, (F) F3 in room temperature (25°C).

**Figure 5.** PLM photography of dispersed formulations ( $\times 1000$ ). (A) F3, (B) F18, (C) F13, (D) F14. Arrows show examples of anisotropic forms of LLC (hexosomes, lamellar), the black background is formed of isotropic LLC (cubosomes)

**Figure 6.** TA release from dispersed LLC formulations. F3 (3.5% w/w GMO), F13 (6.3% w/w GMO), F14 (2.5% w/w GMO, 1% w/w PC), F18 (with 0.25% w/w HP $\beta$ CD)

### Table Captions

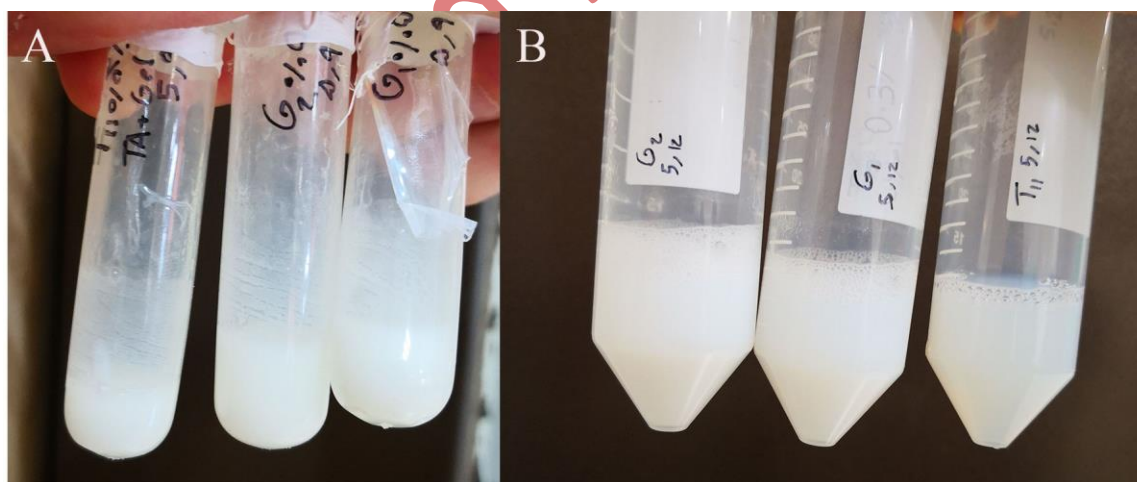
**Table 1.** Composition of dispersed LLC formulations containing TA

**Table 2.** Particle size, size distribution, and zeta potential of dispersed LLC formulations.

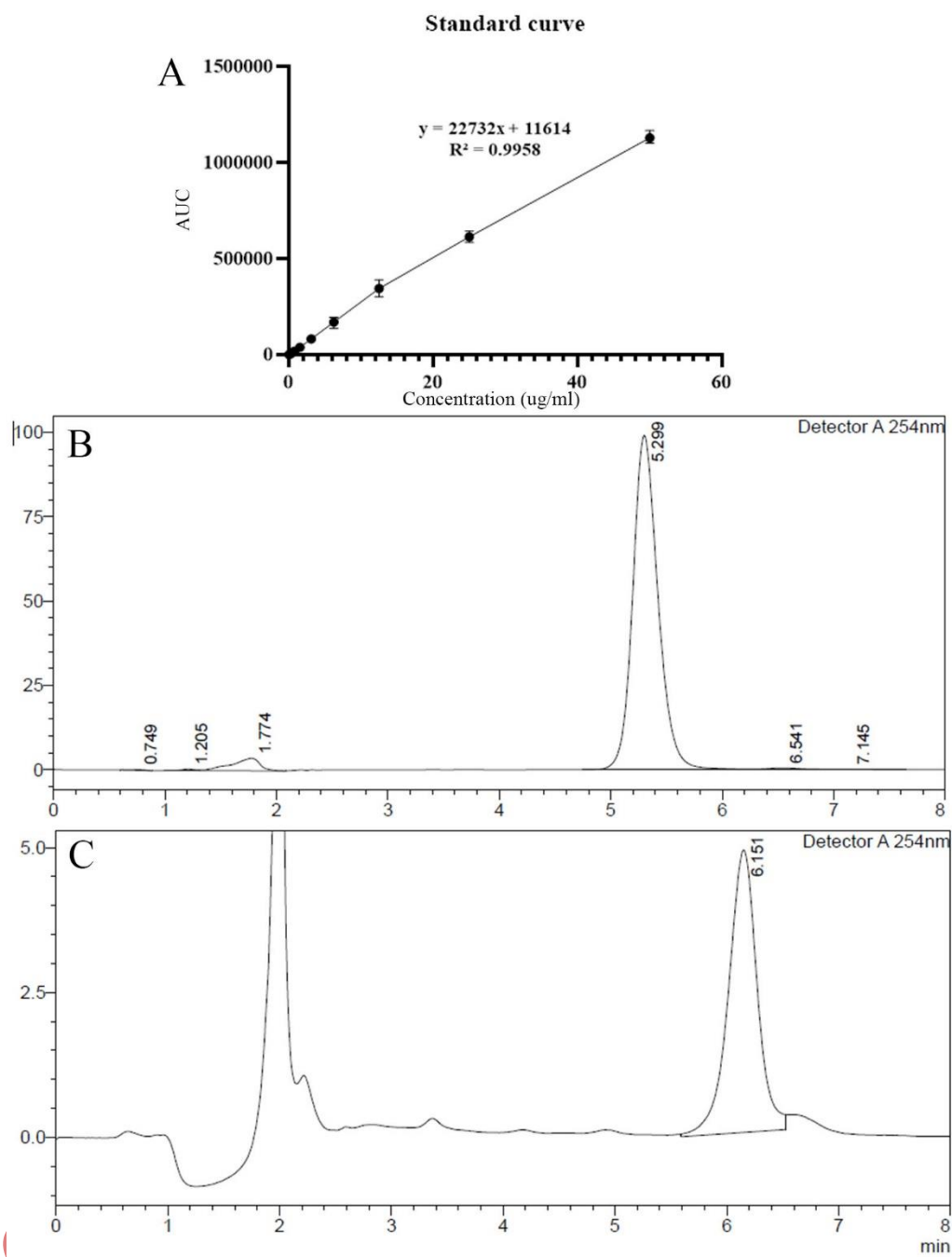
**Table 3.** Loading and Encapsulation efficacy of dispersed formulations.

**Table 4.** Similarity factor ( $f_2$ ) for TA release comparison.

**Table 5.** Comparison of Similarity factor ( $f_2$ ) in the first 6 hours of TA release using ANOVA.



**Figure 1**

**Figure 2**



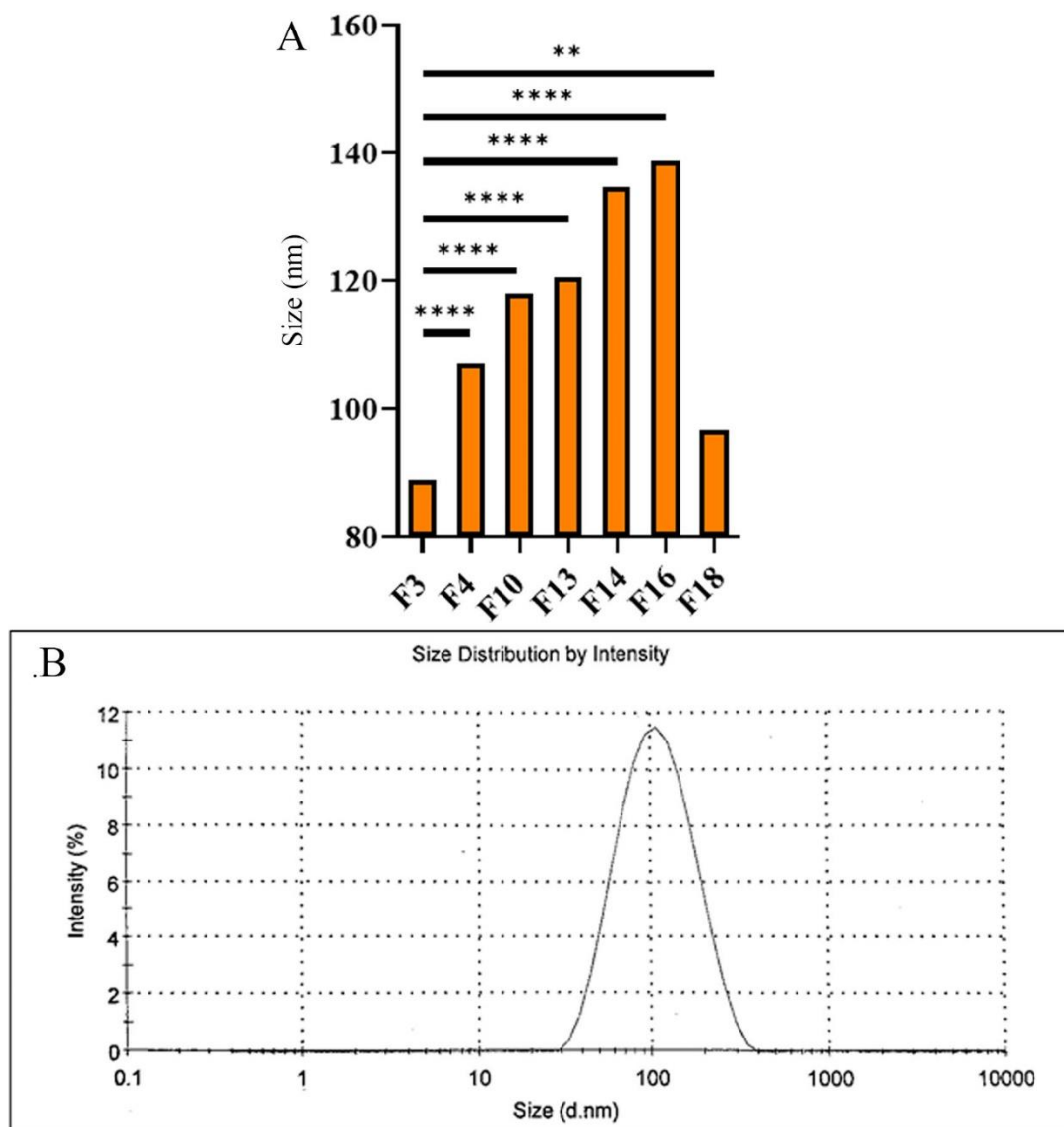


Figure 3

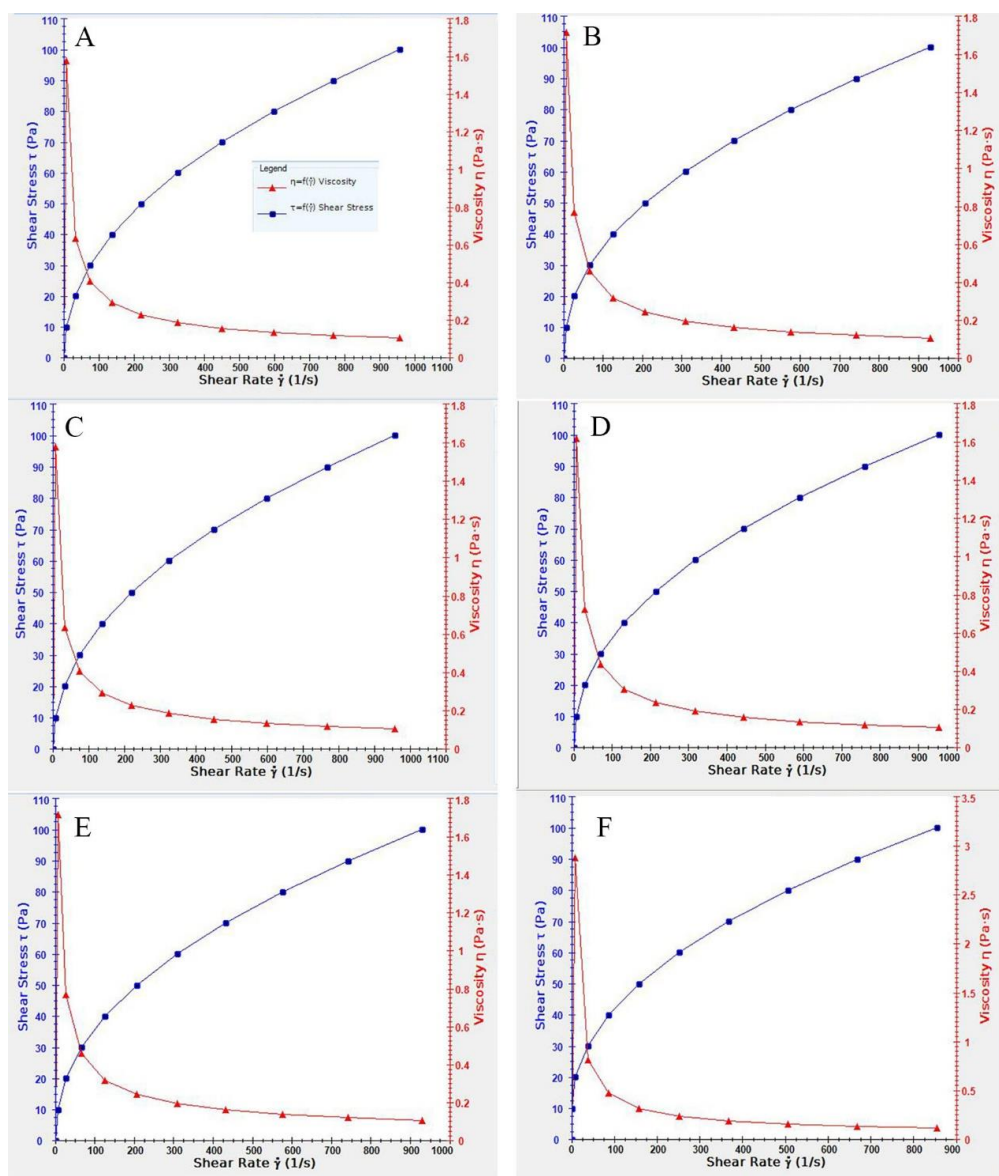


Figure 4

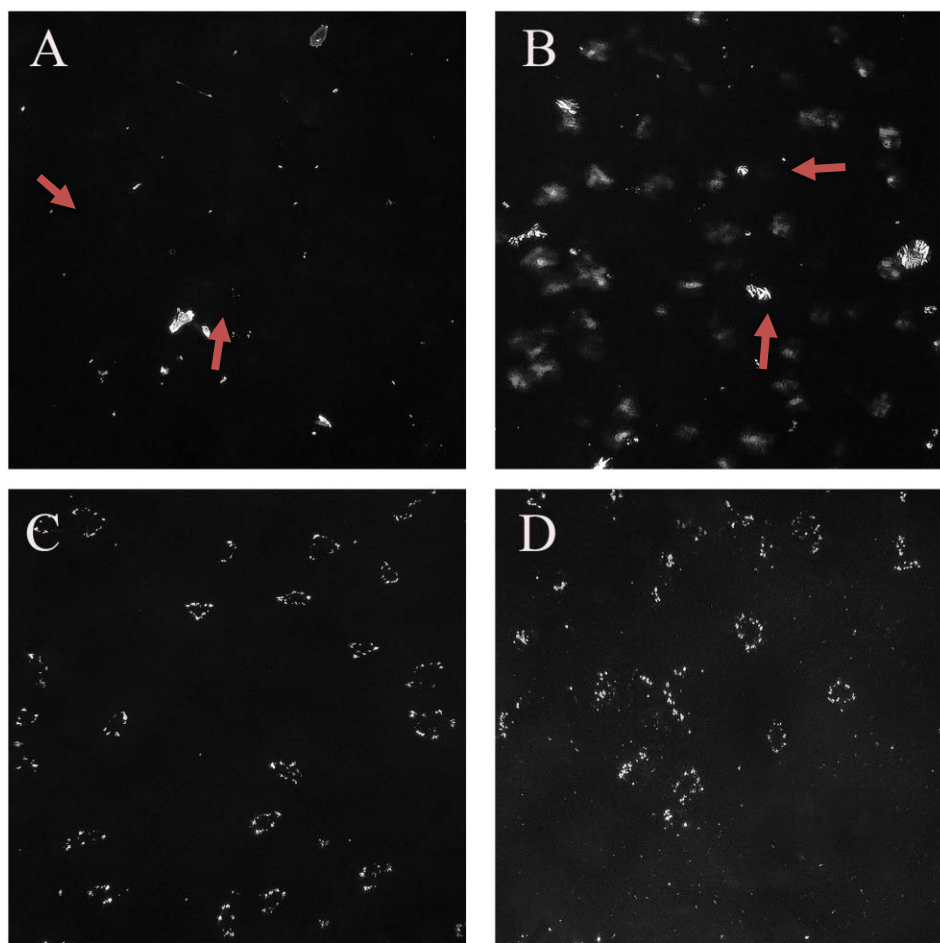


Figure 5

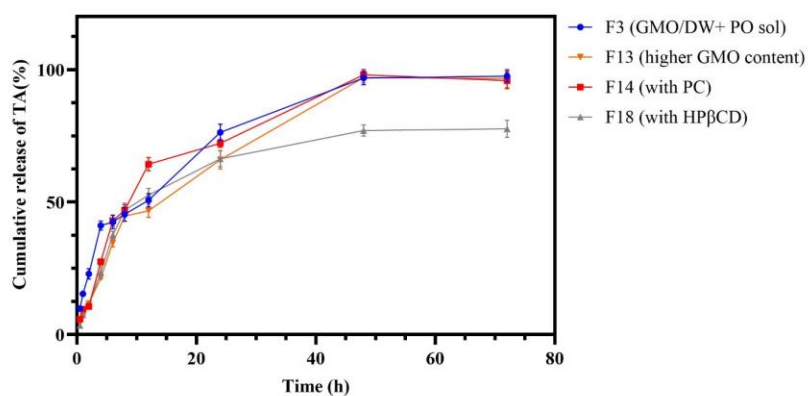


Figure 6

Table 1.

Formulation	TA concentration	Content(w/w%)			
		GMO	PO sol	DW	Other content
F1	0.4% w/w	3.5	95	1.5	
F2	0.4% w/w		99.6		
F3	0.05% w/w	3.5	95	1.5	
F4*	0.05% w/w	3.5	95	1.5	
F5*	0.07% w/w	3.5	95	1.5	
F6*	0.1% w/w	3.5	95	1.5	
F7*	0.2% w/w	3.5	95	1.5	
F8*	0.3% w/w	3.5	95	1.5	
F9*	0.1% w/w	3.5	95	1.5	
F10	0.3% w/w	3.5	95	1.5	
F11	0.03% w/w	3.5	95	1.5	
F12	0.05% w/w	4.9	93	2.1	
F13	0.05% w/w	6.3	91	2.7	
F14	0.05% w/w	2.5	95	1.5	1% PC
F15	0.05% w/w	1.5	95	1.5	2%PC
F16	0.05% w/w	4	93	2	1%PC
F17	0.05% w/w	3.47	94.4	1.49	0.61% HP $\beta$ CD
F18	0.05% w/w	3.49	94.76	1.49	0.25% HP $\beta$ CD

Abbreviations: TA, Triamcinolone acetoneide, GMO, glycerin monooleate, PO, pluronic F127 GEL, lipid liquid crystal gel, HP $\beta$ CD, Hydroxypropyl- $\beta$ -cyclodextrin, DW, deionized water Formulations marked by \* were prepared using a different method as described.

Table 2.

Formulation	Z. Average (nm)	PDI	Zeta potential (mV)
F3 (0.05%)	89.01 $\pm$ 0.21	0.217 $\pm$ 0.021	-20.7 $\pm$ 0.4
F4 (0.05%)	107.04 $\pm$ 0.14	0.256 $\pm$ 0.009	-25.5 $\pm$ 0.1
F10 (0.3%)	118.10 $\pm$ 0.09	0.312 $\pm$ 0.015	-38.5 $\pm$ 0.8
F13 (0.05%)	134.82 $\pm$ 0.20	0.238 $\pm$ 0.030	-16.4 $\pm$ 0.3
F14 (0.05%)	138.73 $\pm$ 0.14	0.355 $\pm$ 0.102	-32.8 $\pm$ 0.2
F16 (0.05%)	141.10 $\pm$ 0.31	0.356 $\pm$ 0.081	-28.4 $\pm$ 0.3
F18 (0.05%)	96.70 $\pm$ 0.18	0.202 $\pm$ 0.041	-14.3 $\pm$ 0.5

Table 3.

Formulation	Drug content (mg)	Loading (%)	EE (%)
<b>F3</b>	1.85	0.0185 $\pm$ 0.031	37.05 $\pm$ 0.05
<b>F3 sediment</b>	1.20	-	-
<b>F13</b>	1.50	0.0150 $\pm$ 0.052	30.10 $\pm$ 0.12
<b>F13 sediment</b>	3.63	-	-
<b>F14</b>	1.36	0.0136 $\pm$ 0.048	27.22 $\pm$ 0.08
<b>F14 sediment</b>	1.03	-	-
<b>F18</b>	2.10	0.0210 $\pm$ 0.104	42.31 $\pm$ 0.14
<b>F18 sediment</b>	1.43	-	-



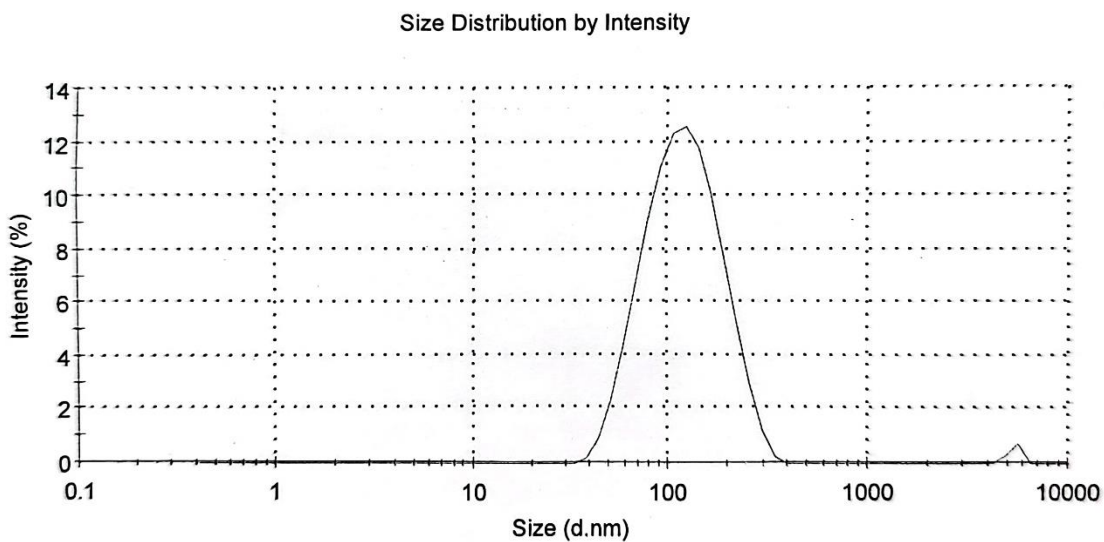
**Table 4.**

Time (h)	f2 (F18-F13)	f2 (F14-F18)	f2 (F14-F18)	f2 (F3-F13)	f2 (F3-F18)	f2 (F3-F14)
0.5	95.57	85.92	79.72	65.74	62.83	74.30
1	91.36	73.25	81.04	52.14	54.94	61.77
2	99.31	89.86	92.60	47.33	46.85	45.07
4	78.41	60.26	71.14	35.39	38.37	43.56
6	69.55	52.81	65.52	54.94	69.43	94.33
8	73.74	75.50	99.21	85.34	87.12	89.96
12	73.30	40.29	45.38	88.63	83.31	42.27
24	99.99	80.97	80.85	56.61	56.56	64.11
48	33.58	99.37	33.83	97.25	33.04	94.83
72	33.89	94.93	34.71	99.94	33.97	95.65

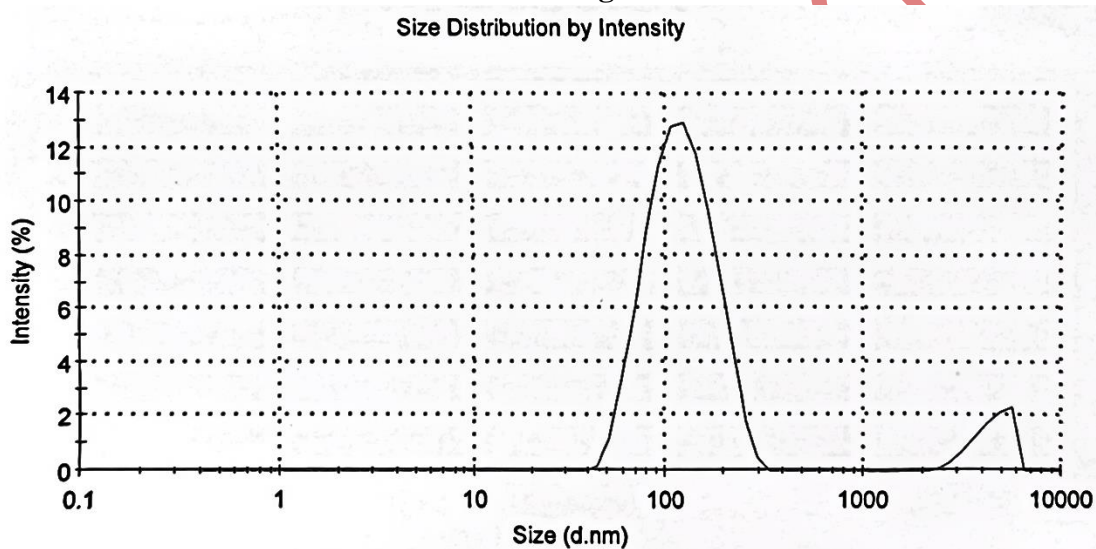
**Table 5.**

Tukey's multiple comparisons test	Mean Diff.	95.00% CI of diff.	Adjusted P value	Summary
f2(F3-F14) vs. f2(F3-F18)	9.326	-18.84 to 37.49	0.9053	ns
f2(F3-F14) vs. f2(F3-F13)	12.70	-15.47 to 40.87	0.7301	ns
f2(F3-F14) vs. f2(F14-F18)	-14.20	-42.36 to 13.97	0.6321	ns
f2(F3-F14) vs. f2(F14-F13)	-8.611	-36.78 to 19.56	0.9304	ns
f2(F3-F18) vs. f2(F3-F13)	3.372	-24.79 to 31.54	0.9990	ns
f2(F3-F18) vs. f2(F14-F18)	-23.52	-51.69 to 4.646	0.1406	ns
f2(F3-F18) vs. f2(F18-F13)	-32.36	-60.53 to -4.192	0.0179	*
f2(F3-F13) vs. f2(F14-F13)	-21.31	-49.48 to 6.858	0.2177	ns
f2(F3-F13) vs. f2(F18-F13)	-35.73	-63.90 to -7.565	0.0075	**
f2(F14-F18) vs. f2(F14-F13)	5.584	-22.58 to 33.75	0.9890	ns
f2(F14-F18) vs. f2(F18-F13)	-8.83	-37.01 to 19.33	0.9229	ns

**Appendix I****Size distribution diagram of other dispersed LLC formulation**

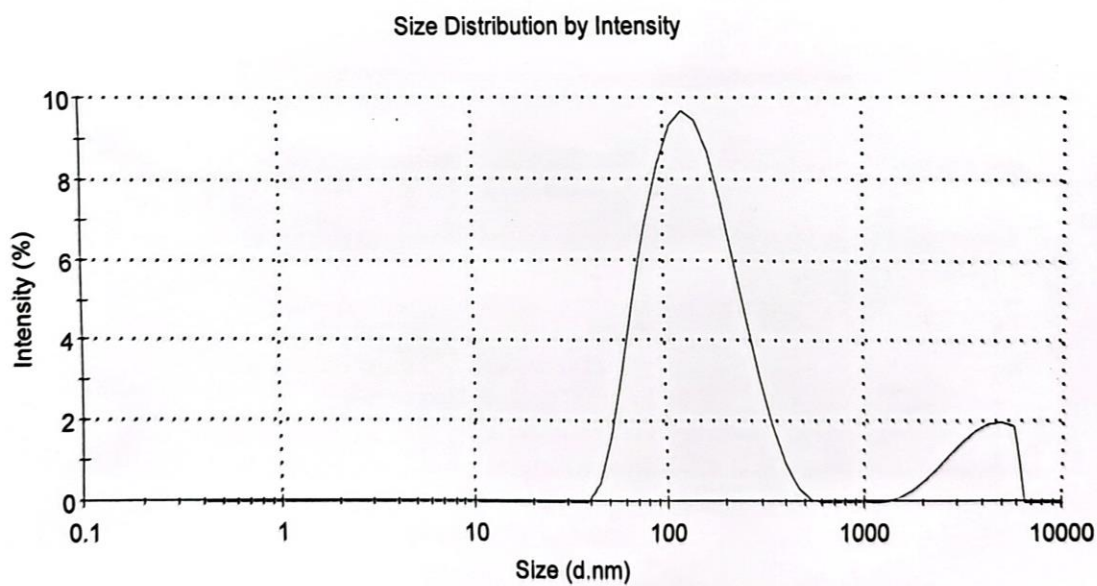


Size distribution diagram of F4

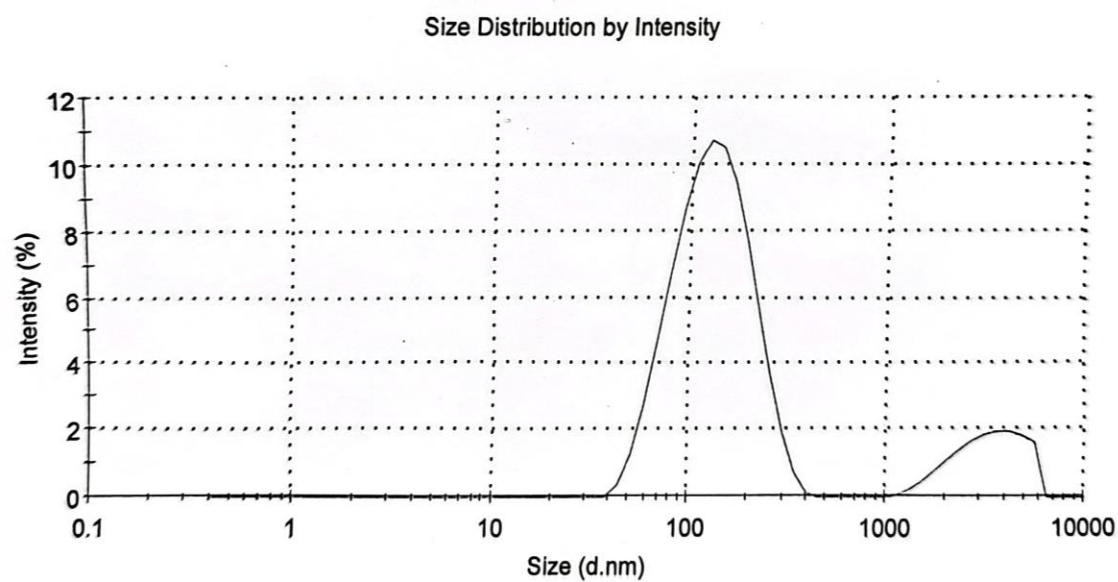


Size distribution diagram of F10

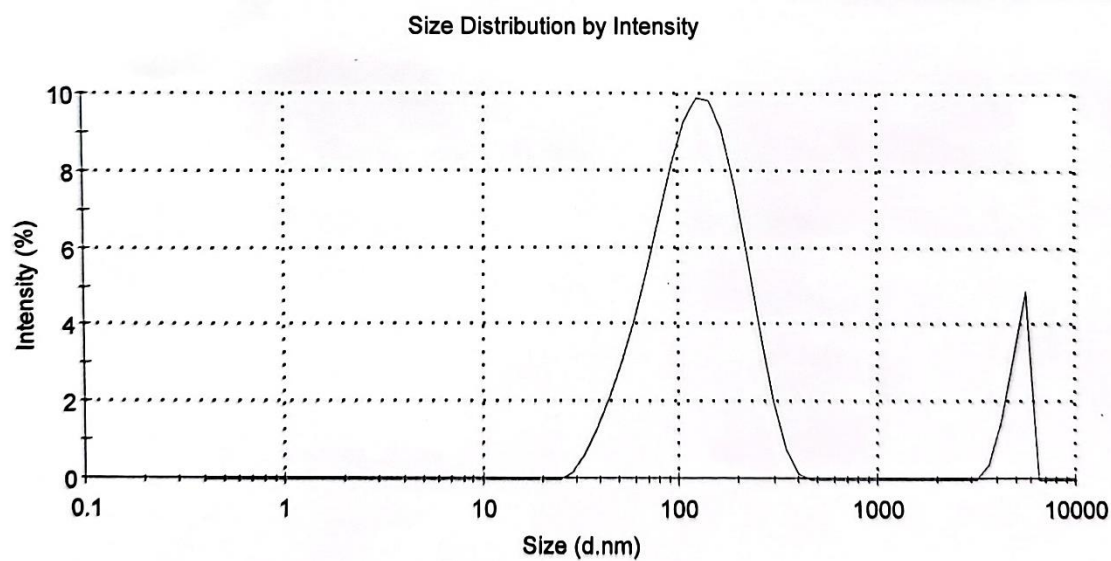
ACCEPTED



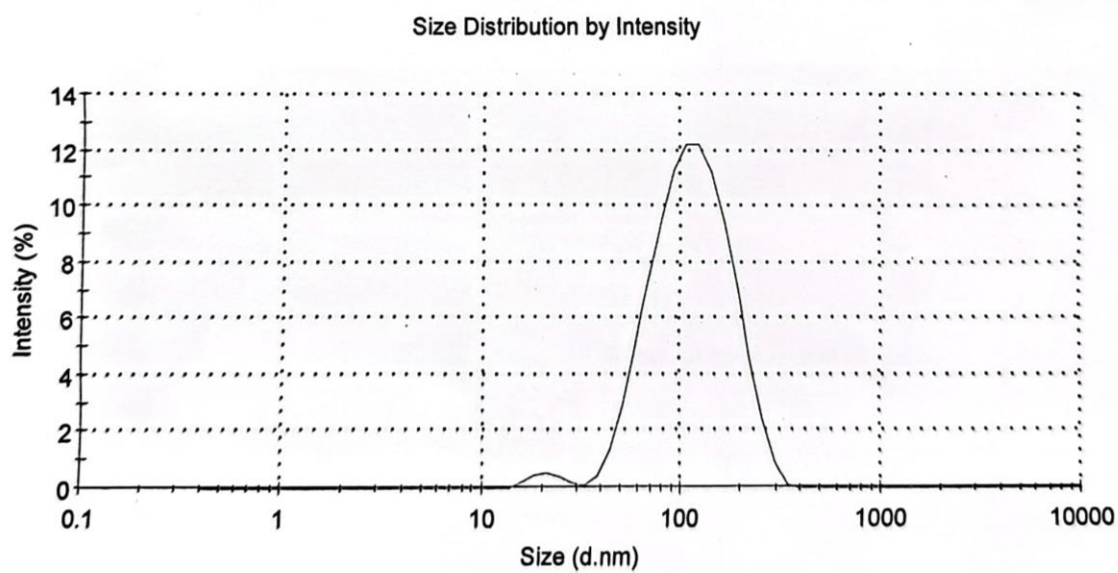
**Size distribution diagram of F13**



**Size distribution diagram of F14**



Size distribution diagram of F16



Size distribution diagram of F18